



Original research

Development of a clot-adhesive coating to improve the performance of thrombectomy devices

Charles Skarbek ,¹ Vania Anagnostakou ,² Emanuele Procopio,¹ Mark Epshtein ,² Christopher M Raskett,² Romeo Romagnoli,³ Giorgio Iviglia,⁴ Marco Morra,⁴ Marta Antonucci,⁵ Antonino Nicoletti,^{1,6} Giuseppina Caligiuri ,^{1,7} Matthew J Gounis ²

► Additional supplemental material is published online only. To view, please visit the journal online (<http://dx.doi.org/10.1136/jnis-2022-019779>).

For numbered affiliations see end of article.

Correspondence to

Dr Giuseppina Caligiuri, U1148 Laboratory for Vascular Translational Science (LVTS), INSERM, Paris 75877, France; giuseppina.caligiuri@inserm.fr

CS and VA contributed equally. GC and MJG contributed equally.

Received 28 October 2022
Accepted 18 February 2023

ABSTRACT

Background The first-pass complete recanalization by mechanical thrombectomy (MT) for the treatment of stroke remains limited due to the poor integration of the clot within current devices. Aspiration can help retrieval of the main clot but fails to prevent secondary embolism in the distal arterial territory. The dense meshes of extracellular DNA, recently described in stroke-related clots, might serve as an anchoring platform for MT devices. We aimed to evaluate the potential of a DNA-reacting surface to aid the retention of both the main clot and small fragments within the thrombectomy device to improve the potential of MT procedures.

Methods Device-suitable alloy samples were coated with 15 different compounds and put in contact with extracellular DNA or with human peripheral whole blood, to compare their binding to DNA versus blood elements in vitro. Clinical-grade MT devices were coated with two selected compounds and evaluated in functional bench tests to study clot retrieval efficacy and quantify distal emboli using an M1 occlusion model.

Results Binding properties of samples coated with all compounds were increased for DNA (≈ 3 -fold) and decreased (≈ 5 -fold) for blood elements, as compared with the bare alloy samples in vitro. Functional testing showed that surface modification with DNA-binding compounds improved clot retrieval and significantly reduced distal emboli during experimental MT of large vessel occlusion in a three-dimensional model.

Conclusion Our results suggest that clot retrieval devices coated with DNA-binding compounds can considerably improve the outcome of the MT procedures in stroke patients.

INTRODUCTION

Despite several effective preventive strategies, stroke remains a leading cause of permanent disability.¹ In the settings of acute intracranial large vessel occlusions, the current generation of mechanical thrombectomy (MT) devices has been associated with a significant clinical benefit.^{2–3} However, MT procedures carry the risk of iatrogenic clot fragmentation and embolism of the distal vascular bed, defined as secondary embolism (SE), or even emboli to a new territory

WHAT IS ALREADY KNOWN ON THIS TOPIC

⇒ New mechanical thrombectomy devices are being improved continuously by design elements to increase the mechanical interaction with clot. However, there is little research to study chemical surface modifications specifically targeting the structure or composition of the clot.

WHAT THIS STUDY ADDS

⇒ The design of a chemical surface modification of the device opens the way for a specific targeting tool to increase the interaction with the clot on a molecular level.

HOW THIS STUDY MIGHT AFFECT RESEARCH, PRACTICE OR POLICY

⇒ This new surface modification, which can be applied to all commercially available mechanical thrombectomy devices, leads to binding of neutrophil extracellular traps and a decrease in distal embolization.

(ENT). Such SE or ENT may unfavorably influence clinical outcome.⁴ Various strategies have been employed to reduce SE rates, including the design refinement of MT devices and the study of their effectiveness to interact with the clot.^{5–7} The latter would be favored by devices able to selectively adhere to clot-enriched components but not to flowing blood elements. In this setting, recent studies have extensively described the presence of neutrophil extracellular traps (NETs), dense meshes of extracellular DNA, consistently found around and inside the retrieved clots.^{8,9} We therefore hypothesized that engrafting of DNA-binding compound on the surface of MT device struts might improve their ability to adhere to clots and retain released clot fragments, through the binding of the associated DNA meshes. In the present study, we have screened the potential of 15 known DNA-binding compounds in terms of specific capture of extracellular DNA versus non-specific stickiness to blood components when immobilized on device-suitable alloy discs in vitro. Then, the performances of clinical-grade, surface-modified, stent retrievers in a simulated



© Author(s) (or their employer(s)) 2023. Re-use permitted under CC BY-NC. No commercial re-use. See rights and permissions. Published by BMJ.

To cite: Skarbek C, Anagnostakou V, Procopio E, et al. *J NeuroIntervent Surg* Epub ahead of print: [please include Day Month Year]. doi:10.1136/jnis-2022-019779

in vitro middle cerebral artery (MCA) occlusion model were evaluated.¹⁰

MATERIAL AND METHODS

All procedures described below are demonstrated in a diagram that can be found in the supplementary materials (online supplemental information S1).

Material

Nitinol (NiTi) flat discs (4.8 mm diameter, 0.25 mm thick) were laser cut and mirror polished by a controlled industrial workshop (Vuichard Michel SAS, Dingy-en-Vuache, France) from a flat NiTi ribbon (5 mm diameter, 0.25 mm thick, Goodfellow Cambridge Ltd, Huntingdon, UK) and were used for the in vitro experiments. For the bench test evaluation, Solitaire devices (6 mm × 20 mm × 180 cm, Medtronic Neurovascular, Irvine, CA) were used.

Surface modification of NiTi material

All NiTi materials were ultrasound cleaned in successive acid, alcohol, and water baths before the functionalization process comprising three successive dip-coating steps, as described in the patent application WO2021EP64257. Briefly, the discs were first immersed in an alkaline solution of dopamine (Alfa Aesar, A11136) for 20±2 hours under stirring, to obtain a thin polydopamine (PDA) film.¹¹ Deionized water washes and ultrasound sonication was applied to withdraw PDA aggregates before immersion in the second bath, aimed at grafting an amine functionalized-cyclooctyne derivative anchor (DBCO-Sulfo-PEG(4)-NH₂, IRIS biotech GMH) on the free catechol group from the PDA film. After extensive washing with deionized water, the final step led to the immobilization of an azide derivative of each compound of interest, through a bio-orthogonal alkyne-azide copper-free click-chemistry reaction.¹² Uniform coating of the medical grade MT devices, Solitaire devices, was achieved using an automatic dip-coater (ND-DC, Nadetech, Navarra, Spain). Once coated, the medical devices were soaked in absolute ethanol for 1 min, left to dry and resheathed before the experiments.

Surface modification characterization

Surface modification of the flat samples was characterized by X-ray photoelectron spectroscopy (XPS), atomic force microscopy (AFM), and ζ-potential measurement, as detailed in the online supplemental material.

Evaluation of the binding to extracellular chromatin versus circulating blood platelets

Chromatin and platelet binding evaluation were studied as described in the patent application WO2021EP64257¹³ and detailed in the online supplemental material. Briefly, the amount of captured extracellular DNA or blood platelets was quantified by computer-assisted analysis of fluorescence microscopy images. The ability of coated surfaces to bind extracellular DNA was evaluated by applying the active surface of the experimental discs stained with the cell impermeant nuclear dye Sytox Green (S7020, Invitrogen, France) on a 3 min contact with human neutrophils stimulated with nigericin (which triggers the formation of NETs).¹⁴

Immersion in fresh whole peripheral human blood for 10 min, followed by an incubation with DAPI (4',6-diamidino-2-phenylindole) and fluorescent antibodies

directed against glycoporphin and CD61, allowed quantification of adhering blood leukocytes, erythrocytes, and platelets.

Functional bench assay: MCA occlusion model

These experiments were performed by an experienced interventional neuroradiologist (VA) and aimed to evaluate the effect of surface-modified Solitaire devices compared with un-modified bare metal stents (BMS) in terms of clot retrieval and SE decrease. The model reproduces the conditions of an MCA occlusion.^{10 15} The clot used in these experiments was prepared using thrombin-induced clotting of bovine blood, and experimental clots were incubated at 37°C for 48 hours before use. The latter steps favored the formation of extracellular traps within the experimental clots.

Before initiating thrombectomy, complete vessel occlusion with a modified Thrombolysis In Cerebral Infarction (mTICI) score of 0 was confirmed by angiography and MCA flow measurements. Each Solitaire was deployed at the occlusion site and remained in place for 3 min before retrieval. Clot fragments generated during MT were collected into two collection reservoirs (one for SE to the MCA distribution and the other for ENT to the anterior cerebral artery distribution). The entire procedure is detailed in online supplemental material.

Surface-modified Solitaire devices included stents coated with MBF (mustard benzo[b]furan, a DNA mustard derivative) and Pipe-2. BMS and PDA-coated devices were used as controls.

Ten experiments were carried out for each group (BMS, PDA, MBF and Pipe-2). The maximum number of passes (thrombectomy attempts) was limited to three. All stents were randomized, numbering them from 1 to 40. Briefly, an AXS Catalyst 5F (Stryker, MI) aspiration catheter connected to a Penumbra aspiration pump (Alameda, CA) was used as an adjunctive thrombo-aspiration procedure in all experiments. The aspiration catheter was advanced over the microcatheter with the stent retriever deployed. Aspiration was initiated with the catheter positioned at the proximal end of the deployed stent and the catheter advanced until flow through the tubing ceased. During the thrombectomy, the aspiration catheter, microcatheter and stent retriever were locked as a system and withdrawn together.

RESULTS

Surface modification characterization

Surface modification characterization of uncoated and functionalized NiTi disc: PDA, PDA-DBCO (dibenzocyclooctyne) and PDA-DBCO-ligand were achieved using XPS to evaluate the chemical organization, and AFM to evaluate the microscopic modification. XPS analyses are reported in table 1. BMS samples had the expected peaks of Ti, Ni, O and C (data not shown). The surface chemistry of coated samples was instead completely

Table 1 Surface organic composition of modified device-suitable alloys detected by XPS (mean±SD)

	PDA	PDA+DBCO	PDA+DBCO+ligand
C	72.3±0.3	70.0±0.7	71.0±0.4
O	20.9±0.3	22.6±0.6	20.5±0.4
N	6.9±0.2	7.3±0.6	8.3±0.8
S	NA	NA	0.3±0.1
O/C	0.29	0.32	0.29
N/C	0.10	0.10	0.12

C, Carbon; DBCO, dibenzocyclooctyne; N, Nitrogen; NA, not applicable; O, Oxygen; PDA, polydopamine; S, Sulfur; XPS, X-ray photoelectron spectroscopy.

organic, showing strong C, O, and N peaks. As expected, the deposited PDA coating was laterally homogeneous and vertically thicker than XPS sampling depth, about 8 nm, in agreement with published data.^{16,17} Its elemental percent was in accordance with published data,¹⁶ the same way the N/C ratio of 0.10 was also in agreement with the expected value. Coupling of DBCO yielded a slight increase of the O/C ratio reflecting the chemistry of the DBCO spacer arm, which contains polyethylene glycol (PEG)—CH₂CH₂O—repeating units. After ligand coupling, further slight modification of surface stoichiometry was observed and coherent with the immobilization of a new chemical and indicated successful coupling of the ligand.

Non-contact AFM analyses are reported in online supplemental information S3. Uncoated NiTi discs showed the presence of a flat surface with a slight difference in the morphology through AFM analysis. PDA coupling led to a classic spot morphology on the surface,^{17,18} which was uniformly distributed. Scanning electron microscopy images confirmed the presence of spherical particles on the PDA surface (data not shown). Adding DBCO followed by the final addition of the ligand did not modify the morphology of the surface. The measurement in three random regions of interest of final surface profile (online supplemental information S4) demonstrated a symmetrical profile of the surface modification with respect to the mean line.

The contact between a solid surface and a water-based medium leads to the development of a surface charge (ζ -potential) at the interface. This charge is one of the surface characteristics which could affect the interaction between the material and the biological environment. In particular ζ -potential was measured as a function of pH, in the 4.5–8.5 range, in 1 mM potassium chloride solution (online supplemental information S5). In the case of bare NiTi, the pH scan is typical of a very weak acid-base interfacial activity and it is driven by pH dependent adsorption of ions. Addition of PDA shows a negative surface which is due to the presence of more phenolic groups exposed on the surface than amine. The presence of DBCO does not change the surface charge significantly; however, the presence of ligand makes the surface potential higher in value and much more negative, which may be due to the exposition of the carboxylic group which makes the surface of the material more acidic.

Evaluation of the chromatin and blood elements binding

As the main goal is to target chromatin mesh composing acute ischemic stroke thrombi, we focused on the coating of the discs with well-known chromatin interacting compounds already used in clinical routine for various applications. The binding property to chromatin and stickiness to blood platelets of 15 DNA interacting agents was studied, considering their toxicity, scalability and manufacturing cost (online supplemental information S6). Pipe-2 (piperazine derivative) and MBF-coated samples showed the most interesting results with regard to both platelet

and chromatin binding compared with bare NiTi discs. The binding data are summarized in table 2. PDA-coated discs were also evaluated to assess the binding properties of the polymer film alone. All fully coated discs demonstrated increased binding to chromatin and a low platelet adhesion compared with the bare discs (ratio 0.27), with the ratio ranging from 0.67 to 6.62. The best results were obtained for the MBF compound with a nearly threefold increase in chromatin binding affinity and almost a fivefold decrease in platelet adhesion as compared with the bare discs. Pipe-2 also showed interesting results with a good affinity for chromatin compared with platelet (ratio of 2.27). On the other hand, PDA coating demonstrated similar specificity for chromatin and platelet binding as compared with bare metal discs. Leukocytes and erythrocytes were virtually absent from all samples.

First pass recanalization and mTICI score

All devices achieved complete recanalization (mTICI 3) after a maximum of three passes (figure 1). BMS and the MBF coated device showed higher rates of first-pass recanalization with mTICI 3 in 100% of cases, compared with PDA (seven out of 10 experiments, 70%) and Pipe-2 (nine out of 10 experiments, 90%) coated devices (not significant). Higher numbers of passes were required to achieve complete recanalization in the PDA group compared with the other devices, but no significant differences among devices were seen. The clot detachment from the device is plotted in figure 1 and shows an important clot detachment in the BMS group (70% of case) compared with the MBF, PDA and Pipe-2 groups in which clot detached in 20%, 20% and 10% of cases, respectively (representative examples in online supplemental information S7).

Secondary embolism

SE rates were increased in the BMS group for each macro- and microemboli, as well as overall total count of distal emboli (table 3). The total count of macroemboli, characterized as large clot fragments >1000 μ m, was higher for the BMS (29 macroemboli) as compared with the coated devices in which 19, eight, and 18 macroemboli were recorded in the PDA, MBF, and Pipe-2 groups, respectively. The mean number of macroemboli per experiment is illustrated in figure 1. A statistically significant difference was found for the MBF group compared with BMS (P=0.0211).

The total count of microemboli, characterized as clot fragments ranging from 200 μ m to 1000 μ m, was similar in the BMS and PDA groups with 26 and 30 microemboli recorded, respectively. MBF and Pipe-2 groups showed a decrease in microemboli count compared with BMS and PDA (11 and seven microemboli, respectively). There were no statistically significant differences in the number of macroemboli observed in either coated group compared with BMS (figure 1). Finally, the overall count of distal emboli (including micro- and macroemboli) was higher in the BMS (55 distal emboli) and PDA coated devices (49 distal emboli) compared with MBF (19 distal emboli) and Pipe-2 (25 distal emboli) coated devices (figure 1). A statistically significant difference was found for the MBF and Pipe-2 coated devices group compared with BMS (P=0.0418 and 0.0416, respectively).

DISCUSSION

Despite the tremendous advances in the design of new MT devices in the past decades,^{19,20} the MT procedure may still be optimized. In spite of radiological success in about 80% of the interventions, a completely positive clinical outcome is realized

Table 2 Binding properties of chromatin and platelets (mean \pm SEM)

Ligand	Chromatin binding (% of max)	Platelet binding (% of max)	Chromatin/platelet binding ratio
Bare metal	29.69 \pm 8.63	90.71 \pm 1.54	0.27
PDA	24.57 \pm 8.50	36.32 \pm 5.45	0.67
MBF	66.07 \pm 13.21	9.98 \pm 3.37	6.62
Pipe-2	44.23 \pm 10.64	19.45 \pm 3.90	2.27
MBF, mustard benzo[b]furan, a DNA mustard derivative; PDA, polydopamine; Pipe-2, piperazine derivative.			

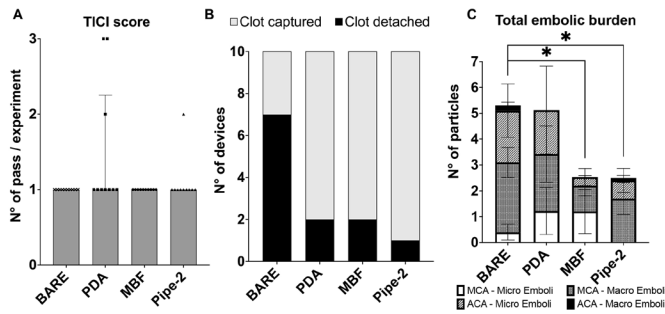


Figure 1 Number of passes to achieve mTICI score of 3 (A), clot capture versus detachment (B), and total embolic burden (number of particles released during the procedure, average±SD), according to the tested group (C). n=10/group, *P<0.05. BARE, bare metal stent; ACA: anterior cerebral artery; MBF, mustard benzo[b]furan, a DNA mustard derivative; MCA, middle cerebral artery; mTICI, modified Thrombolysis In Cerebral Infarction; PDA, polydopamine; Pipe-2, piperazine derivative.

in only half of the procedures.²¹ In addition, Wong *et al* documented the issue of SE or ENT which occurs in about 40% of cases.⁴ Lastly, Luraghi *et al* described the clot rolling phenomenon during MT that resulted in the detachment of the thrombi from the device during the procedure.²² A recent translational study suggests that thrombectomy outcome would be significantly improved by strategies aimed at increasing the incorporation of the embolus within the device and at minimizing the release of SE or ENT.²³ The quest for a surface modification able to selectively adhere the device to the clot structure, and not the components of the flowing blood, led us to exploit the extracellular chromatin material (only present in blood in very small quantities) that accumulates within and around occlusive thrombi,²⁴ likely due to the local hemodynamic stress consistently found in the clot retrieved from stroke patients.⁹

Here, we report that the immobilization of DNA-binding compounds, through a scalable surface modification process applicable to any commercially available thrombectomy device, can effectively improve the adherence of the occlusive clot to the thrombectomy device, while decreasing the release of secondary emboli in a three-dimensional phantom bench model of acute cerebral artery occlusion.¹⁰

Several compounds are known to interact with DNA, yet our in vitro data indicate that some of them were weaker binders of extracellular chromatin, likely according to the compound nature. The selection of the candidate for our purposes was guided by the best adhesiveness shown within the relatively short contact time (3 min), and this criterion was meant to match the time allowed between the stent deployment and its retrieval during MT procedures in clinical practice. Among all the tested compounds, MBF, Pipe-2 and Pipe-4 showed in vitro the highest capture affinity to DNA.

Table 3 Total count of distal emboli released during the whole study (n=10) according to the tested group

	BMS	PDA	MBF	Pipe-2
Overall macroemboli	29	19	8	18
Overall microemboli	26	30	11	7
Overall distal emboli	55	49	19	25

BMS, bare metal stent; MBF, mustard benzo[b]furan, a DNA mustard derivative; PDA, polydopamine; Pipe-2, piperazine derivative.

Functional tests in the bench model of cerebral artery phantom occlusion effectively showed a superiority of the modified devices in terms of clot incorporation. Indeed, the main clot readily detached from the BMS in seven out of the 10 independent experiments, whereas this occurred in a minority of the experiments performed with the coated devices (2/10, 2/10 and 1/10 with PDA, Pipe-2 and MBF devices, respectively). This observation is consistent with the study by Luraghi *et al* describing the clot rolling phenomenon during the MT when using an in vitro model and a variety of commercial BMS devices.²² Interestingly, most of the tested compounds also showed a reduced (at least a twofold decrease) binding to blood platelets as compared with the control BMS. This finding further demonstrates that the clot-capture property conferred by our surface modification is specific and supports a safer use of the modified device through the arterial bed (reduced risk of platelet aggregation onto the stent retriever). In this perspective, the mere coating with PDA, which we used as an intermediate functionalization layer, could have been proposed as a candidate for its well-known adhesive property.²⁵⁻²⁷ Our data, however, clearly show that this ‘sticky’ property does not bring a specific binding towards DNA as compared with blood platelets; the number of total distal emboli per experiment in the PDA group was similar to the BMS, and significantly reduced with the MBF and Pipe-2 surface modifications. This observation confirms and validates the concept that a specific binding to a component enriched in the clot, and absent in the flowing blood, can significantly improve the global performance of the thrombectomy devices.

Our study has limitations. First, this is an in vitro study and further testing is required to characterize the vascular reaction to these coating concepts in vivo. We chose to use co-aspiration during our stent retriever thrombectomy as this is the clinical routine in many practices,²⁸⁻³¹ which may have reduced the amount of distal emboli; however, we believe that since the technique was standardized across all experimental groups the relative differences remain valid. To maintain scientific rigor and reduce variability of technique, a single operator was used and therefore additional validation with multiple operators to ensure generalizability of the data will be performed. Although NETs are consistently present in clots that cause stroke,⁹ the spatial distribution may vary and may not always come into contact with the low porosity stent retriever construct. Finally, as with all medical devices, standard particulate testing to ensure coating integrity has not yet been performed and will be required before clinical translation.

CONCLUSION

Our work has led to the design of a surface modification procedure scalable and applicable to all commercially available MT devices. This work validates the hypothesis that a surface-modified MT device can be an interesting alternative to bare MT devices, as this modification improves the capture of the main clot to decrease the risk of distal embolization.

Author affiliations

- ¹U1148 Laboratory for Vascular Translational Science (LVTS), INSERM, Paris, France
- ²Department of Radiology, New England Center for Stroke Research, UMass Chan Medical School, Worcester, Massachusetts, USA
- ³Department of Chemical, Pharmaceutical & Agricultural Sciences, University of Ferrara, Ferrara, Italy
- ⁴Nobil Bio Ricerche srl, Portacomaro, Italy
- ⁵Cardiovascular Lab SpA, Milan, Italy
- ⁶Université Paris Cité, Paris, France
- ⁷Department of Cardiology, Hôpitaux Universitaires Paris Nord Val-de-Seine, Site Bichat, AP-HP, Paris, Île-de-France, France

Twitter Giuseppina Caligiuri @pinacaligiuri

Contributors CS: study design, data acquisition, data analysis, data interpretation, manuscript preparation. VA: study design, data acquisition, data analysis, data interpretation and revised the draft manuscript. AN, MJG and GC: study design, data analysis, data interpretation, revised the draft manuscript and guarantor. RR: compound derivatization, synthesis, and purification. EP, ME, CMR and RR: data acquisition, data interpretation. GI, MM: data acquisition, data interpretation, manuscript preparation.

Funding This work is supported by a government grant managed by the French National Research Agency (ANR) as part of the future investment program integrated into France 2030, under grant agreement No. ANR-18-RHUS-0001. The 3D Willis phantom bench work was funded by the incubator Cardiovascular Lab S.p.A (CVLab).

Competing interests CS salary is supported by a grant from the French National Research Agency (ANR). GC received research support from the French National Research Agency (ANR) and from the incubator Cardiovascular Lab. CS, GC, MA and AN are the inventors of a pending patent related to this work (WO2021EP64257). GC and AN are the scientific co-founders of a company related to this work (KAPTO Medical). MJG: 1. Consultant on a fee-per-hour basis for Alembic LLC, Astrocyte Pharmaceuticals, Bendit Technologies, Cerenovus, Imperative Care, Jacob's Institute, Medtronic Neurovascular, Mivi Neurosciences, phenox GmbH, Q'Apel, Route 92 Medical, Scientia, Stryker Neurovascular, Stryker Sustainability Solutions, Wallaby Medical; holds stock in Imperative Care, InNeuroCo, Galaxy Therapeutics, Neurogami, and Synchro; 2. Research support from the NIH, the United States–Israel Binational Science Foundation, Anaconda, ApicBio, Arsenal Medical, Axovant, Balt, Cerenovus, Ceretrieve, CereVasc LLC, Cook Medical, Galaxy Therapeutics, Gentuity, Gilbert Foundation, Imperative Care, InNeuroCo, Insera, Jacob's Institute, Magneto, MicroBot, Microvention, Medtronic Neurovascular, MIVI Neurosciences, Nagreiter MDDO, Neurogami, Philips Healthcare, Progressive Medical, Pulse Medical, Rapid Medical, Route 92 Medical, Scientia, Stryker Neurovascular, Syntheon, ThrombX Medical, Wallaby Medical, the Wyss Institute and Xtract Medical; 3. Associate Editor of Basic Science on the JNIS Editorial Board. MM owns shares of the company Nobil Bio Ricerche srl. GI are employees of Nobil Bio Ricerche srl.

Patient consent for publication Not applicable.

Ethics approval Not applicable.

Provenance and peer review Not commissioned; externally peer reviewed.

Data availability statement Data are available upon reasonable request. Examples of the 3D phantom experiments (videos) are provided as supplementary data. All videos are available upon request.

Supplemental material This content has been supplied by the author(s). It has not been vetted by BMJ Publishing Group Limited (BMJ) and may not have been peer-reviewed. Any opinions or recommendations discussed are solely those of the author(s) and are not endorsed by BMJ. BMJ disclaims all liability and responsibility arising from any reliance placed on the content. Where the content includes any translated material, BMJ does not warrant the accuracy and reliability of the translations (including but not limited to local regulations, clinical guidelines, terminology, drug names and drug dosages), and is not responsible for any error and/or omissions arising from translation and adaptation or otherwise.

Open access This is an open access article distributed in accordance with the Creative Commons Attribution Non Commercial (CC BY-NC 4.0) license, which permits others to distribute, remix, adapt, build upon this work non-commercially, and license their derivative works on different terms, provided the original work is properly cited, appropriate credit is given, any changes made indicated, and the use is non-commercial. See: <http://creativecommons.org/licenses/by-nc/4.0/>.

ORCID iDs

Charles Skarbek <http://orcid.org/0000-0003-0054-2064>
 Vania Anagnostakou <http://orcid.org/0000-0001-5101-3192>
 Mark Epshtein <http://orcid.org/0000-0002-1164-7331>
 Giuseppina Caligiuri <http://orcid.org/0000-0003-4973-2205>
 Matthew J Gounis <http://orcid.org/0000-0002-8034-2785>

REFERENCES

- Katan M, Luft A. Global burden of stroke. *Semin Neurol* 2018;38:208–11.
- Yoo AJ, Andersson T. Thrombectomy in acute ischemic stroke: challenges to procedural success. *J Stroke* 2017;19:121–30.

- Appireddy R, Assis Z, Goyal M. Mechanical thrombectomy: new era of stent retriever. In: *Stroke revisited: diagnosis and treatment of ischemic stroke*. 2017: 71–100.
- Wong GJ, Yoo B, Liebeskind D, et al. Frequency, determinants, and outcomes of emboli to distal and new territories related to mechanical thrombectomy for acute ischemic stroke. *Stroke* 2021;52:2241–9.
- Kaneko N, Komuro Y, Yokota H, et al. Stent retrievers with segmented design improve the efficacy of thrombectomy in tortuous vessels. *J Neurointerv Surg* 2019;11:119–22.
- Wenger K, Nagl F, Wagner M, et al. Improvement of stent retriever design and efficacy of mechanical thrombectomy in a flow model. *Cardiovasc Intervent Radiol* 2013;36:192–7.
- Chueh JY, Marosfoi MG, Brooks OW, et al. Novel distal emboli protection technology: the embotrap. *Interv Neurol* 2017;6:268–76.
- Ducroux C, Di Meglio L, Loyau S, et al. Thrombus neutrophil extracellular traps content impair TPA-induced thrombolysis in acute ischemic stroke. *Stroke* 2018;49:754–7.
- Laridan E, Zenorme F, Desender L, et al. Neutrophil extracellular traps in ischemic stroke thrombi. *Ann Neurol* 2017;82:223–32.
- Anagnostakou V, Epshtein M, Kühn AL, et al. Preclinical modeling of mechanical thrombectomy. *J Biomech* 2022;130:110894.
- Hu W, Lu S, Zhang Z, et al. Mussel-inspired copolymer-coated polypropylene mesh with anti-adhesion efficiency for abdominal wall defect repair. *Biomater Sci* 2019;7:1323–34.
- Kim E, Koo H. Biomedical applications of copper-free click chemistry: in vitro, in vivo, and ex vivo. *Chem Sci* 2019;10:7835–51.
- Caligiuri G, Nicoletti A, Antonucci M. 2021:20210527.
- Kenny EF, Herzig A, Krüger R, et al. Diverse stimuli engage different neutrophil extracellular trap pathways. *Elife* 2017;6:e24437.
- Chueh JY, Wakhloo AK, Gounis MJ. Neurovascular modeling: small-batch manufacturing of silicone vascular replicas. *AJNR Am J Neuroradiol* 2009;30:1159–64.
- Zangmeister RA, Morris TA, Tarlov MJ. Characterization of polydopamine thin films deposited at short times by autoxidation of dopamine. *Langmuir* 2013;29:8619–28.
- Lee H, Dellatore SM, Miller WM, et al. Mussel-inspired surface chemistry for multifunctional coatings. *Science* 2007;318:426–30.
- Ball V. Impedance spectroscopy and zeta potential titration of dopa-melanin films produced by oxidation of dopamine. *Colloids and Surfaces A: Physicochemical and Engineering Aspects* 2010;363:92–7.
- Beshchasna N, Saqib M, Kraskiewicz H, et al. Recent advances in manufacturing innovative stents. *Pharmaceutics* 2020;12:349.
- Turc G, Bhogal P, Fischer U, et al. European Stroke organisation (ESO) - European Society for Minimally Invasive Neurological Therapy (ESMINT) guidelines on mechanical thrombectomy in acute ischemic stroke. *J Neurointerv Surg* 2019. 10.1136/neurintsurg-2018-014569 [Epub ahead of print 26 Feb 2019].
- Kleine JF, Wunderlich S, Zimmer C, et al. Time to redefine success? TICI 3 versus TICI 2B recanalization in middle cerebral artery occlusion treated with thrombectomy. *J Neurointerv Surg* 2017;9:117–21.
- Luraghi G, Rodriguez Matas JF, Dubini G, et al. Applicability assessment of a stent-retriever thrombectomy finite-element model. *Interface Focus* 2021;11:20190123.
- Liu Y, Gebregziabher D, Reddy AS, et al. Failure modes and effects analysis of mechanical thrombectomy for stroke discovered in human brains. *J Neurosurg* 2022;136:197–204.
- Yu X, Tan J, Diamond SL. Hemodynamic force triggers rapid netosis within sterile thrombotic occlusions. *J Thromb Haemost* 2018;16:316–29.
- Zandieh M, Hagar BM, Liu J. Interfacing DNA and polydopamine nanoparticles and its applications. *Part Part Syst Charact* 2020;37:2000208.
- Yang Z, Tu Q, Zhu Y, et al. Mussel-inspired coating of polydopamine directs endothelial and smooth muscle cell fate for re-endothelialization of vascular devices. *Adv Health Mater* 2012;1:548–59.
- Lynge ME, van der Westen R, Postma A, et al. Polydopamine -- a nature-inspired polymer coating for biomedical science. *Nanoscale* 2011;3:4916–28.
- Humphries W, Hoyt D, Doss VT, et al. Distal aspiration with retrievable stent assisted thrombectomy for the treatment of acute ischemic stroke. *J Neurointerv Surg* 2015;7:90–4.
- Massari F, Henninger N, Lozano JD, et al. ARTS (aspiration-retriever technique for stroke): initial clinical experience. *Interv Neuroradiol* 2016;22:325–32.
- Maus V, Behme D, Kabbasch C, et al. Maximizing first-pass complete reperfusion with SAVE. *Clin Neuroradiol* 2018;28:327–38.
- McTaggart RA, Tung EL, Yaghi S, et al. Continuous aspiration prior to intracranial vascular embolectomy (CAPTIVE): a technique which improves outcomes. *J Neurointerv Surg* 2017;9:1154–9.

jnis-2022-019779-R1

SUPPLEMENTARY MATERIAL

1 Surface modification characterization

Surface modification of the flat samples was characterized by X-Ray Photoelectron Spectroscopy, Atomic Force Microscopy and ζ - potential measurement..

1.1 X-Ray Photoelectron Spectroscopy

X-ray photoelectron spectroscopy (XPS) analysis was performed using a Perkin Elmer PHI 5600 ESCA system (PerkinElmer Inc., Waltham, Massachusetts, USA) equipped with a monochromatized Al anode operating at 10 kV and 200 W. The diameter of the analyzed spot was 500 μm ; and the analyzed depth 8 nm. The base pressure was maintained at 10^{-8} Pa. The angle between the electron analyzer and the sample surface was 45° . Analysis was performed by acquiring wide-range survey spectra (0–1,000 eV binding energy) and detailed high-resolution peaks of relevant elements. Quantification of elements was accomplished using the software and sensitivity factors supplied by the manufacturer. High-resolution C1s peaks were acquired using a pass energy of 11.75 eV and a resolution of 0.100 eV/step.

1.2 Atomic Force Microscopy

Atomic force microscopy (AFM) was used to explore the surface nanotopography of 4.8 mm diameter machined Grade 4 NiTi discs untreated and treated with PDA (dip-coating step 1), PDA+DBCO (dip-coating step 2) and PDA+DBCO+Ligand (dip-coating step 3). Measurements were performed using an NX10 Park AFM instrument (Park System, Suwon, Korea), equipped with 20-bit closed-loop XY and Z flexure scanners and a noncontact cantilever PPP-NCHR 5M. This instrument implements a True Noncontact™ mode, allowing minimization of the tip–sample interaction, resulting in tip preservation, negligible sample nanotopography modification and reduction of artifacts. On each sample, four different sample size areas were analyzed (20×20 , 10×10 , 5×5 , and 1×1 μm) at a scan rate of 0.1 Hz.

jnis-2022-019779-R1

1.3 ζ -potential measurement

ζ -potential measurements were performed using SurPass 3, equipped with an adjustable gap cell (Anton-Paar GmbH, Graz, Austria). Measurements were conducted on 20×10 mm NiTi plates (NiTi foil 250 μ m thickness, Sigma Aldrich), either uncoated or PDA (dip-coating step 1), PDA+DBCO (dip-coating step 2) and PDA+DBCO+ligand (dip-coating step 3) coated. Measurements were performed in a 1 mM KCl solution, according to *pH scan* method. It consists of the measurement of ζ - potential at different pH, between 4.5 and 8.5. The pH of electrolyte solution was modified automatically by the instruments using a 50 mM HCl and 50 mM NaOH. At each pH point, three measurements were performed in order to conditioning the sample, then the fourth value was taken and reported. All calculations were performed by the instrument software.

2 Evaluation of the binding to extracellular chromatin versus circulating blood platelets

Chromatin and platelet binding evaluation were studied as described in the patent application WO2021EP64257.¹³ Bare and coated NiTi discs were used within one week after their coating. The discs were washed twice with sterile PBS before running the evaluation.

2.1 Extracellular chromatin binding evaluation

The ability of coated surfaces to bind extracellular chromatin was evaluated by applying the active surface of the experimental NiTi discs on the bottom of 48-well plates in which fresh isolated human neutrophils were stimulated with nigericin during three minutes, to trigger the formation of NETs¹⁴. Briefly, neutrophils were isolated using an EasySep™ Direct Human Neutrophil Isolation Kit (Stelcell Technologies, France) from healthy donor whole blood retrieved in ACD tube. Isolated neutrophils (300 000 neutrophils, 300 μ L) were incubated in 48-well plates with nigericin (30 μ M, SML1779, Sigma Aldrich Chimie, France) at 37°C to promote the formation of NETs. After a 4h-incubation period, the plate was shaken 5 min at 400 rpm and centrifuged (5 mins, 500 G). Bare and coated discs were immersed in each well

jnis-2022-019779-R1

and left adhering to NETs for three minutes, selected to mimic the time between the stent deployment and its retrieval during MT in clinical practice. After retrieval of the disc, the discs were washed in PBS and fixed for 10 mins in 4% formalin solution. Adhering extracellular chromatin was then stained with the cell impermeant nuclear dye Sytox Green (S7020, Invitrogen, France). The NiTi discs were mounted face-down on ibidi® dishes, using ProlongGold® (Thermofisher, France) and left to dry overnight. Images were taken with an Axio Observer fluorescence microscope (Zeiss, Rueil Malmaison, France) equipped with an ORCA II Digital CCD camera (Hamamatsu Photonics, Massy, France). Fluorescence microscopy images were analyzed using Image J (National Institutes of Health) software, v1.50i for MacOS. The fluorescent intensity was normalized on the maximum observed intensity to evaluate the mean percentage of binding and compare data among the different surfaces.

2.2 Blood platelet binding evaluation

Coated and bare NiTi discs were immersed in the wells of 48-well plates containing fresh whole peripheral human blood (200 µL) deriving from healthy donors. Blood was withdrawn in PPAK tubes (9-SCAT-II-5, cryopep, France), a thrombin inhibitor suited to accurately evaluate the reactivity of platelets *in vitro*.³² Contact with blood was allowed for 10 minutes, a time interval compatible with the travel of the medical device through the circulation of the patients during MT. After 10 minutes, the samples were washed and adhering platelets were revealed by fluorescence microscopy, following an immunostaining with CD61 antibody conjugated to PE (clone Y2/51, 130-124-881, Miltenyi Biotec, Auburn, CA, USA). Finally, the discs were mounted face-down on ibidi® dishes, using ProlongGold® (Thermofisher, France) and left to dry overnight. Image acquisition and fluorescence density analysis were conducted as described above.

jnis-2022-019779-R1

3 Functional bench assay - MCA occlusion model

These experiments aimed to evaluate the effect of surface-modified Solitaire devices compared to un-modified Solitaire devices (bare metal stent, BMS) in terms of clot retrieval and SE decrease. The model reproduces the conditions of a middle cerebral artery (MCA) occlusion. Surface-modified Solitaire devices included stents coated with PDA, MBF and Pipe-2. BMS were used as controls.

Ten experiments were carried out for each group (BMS, PDA, MBF and Pipe-2). The maximum number of passages (thrombectomy attempts) was limited to 3. All stents were randomized, numbering them from 1 to 40. Briefly, an AXS Catalyst 5F (Stryker, Michigan, USA) aspiration catheter connected to a Penumbra aspiration system (Alameda, California, USA) was used as an adjunctive thrombo-aspiration procedure in all experiments. The model system was composed of a human vascular replica, clot model, and a physiologically relevant mock circulation flow loop.¹⁰

3.1 Vascular model

Twenty vascular replicas of the cerebral circle of Willis were built using magnetic resonance angiograms from 20 healthy patients. Informed written consent was obtained in each case. Such replicas were built using a small-batch manufacturing process previously described.¹⁵ AA core-shell mold was created for silicone infusion (Sylgard 184, Dow Corning, Midland MI). By dissolving the core-shell mold in xylene after silicone curing, a transparent and flexible silicone replica was obtained. To reduce the friction between the device and the silicone replica, the inner wall of the resulting replica was lubricated by coating a layer of LSR topcoat (Momentive Performance Materials, Albany NY).

3.2 Clot formation model

jnis-2022-019779-R1

A model of friable clot of medium stiffness (diameter: 4.3mm) was prepared for device testing using thrombin-induced clotting of bovine blood containing barium sulfate (1 g / 10ml blood), fibrinogen (29.7 mg in 0.7ml saline + 1.8 ml blood/barium mixture) and thrombin (50 NIHU thrombin in 0.5ml saline + CaCl₂ added to 2.5ml blood/barium/fibrinogen mixture). This type of clot is prone to fragmentation during MT and was selected specifically to mimic the worst-case scenario with respect to clot fragmentation. The clot was then incubated at 37°C for 48 hours prior to use to increase the chance of chromatin release within the clot. The presence of extracellular traps was confirmed by DAPI and H3cit staining (**Supplemental information S 2**)

3.3 *Ex vivo cerebral circulation flow loop*

The clot (length: ≈ 1cm) was injected into the flow loop driven by a peristaltic pump via a separate entry close to the silicone replica to form an MCA occlusion as described previously.³³ Briefly, an acrylic box containing the silicone replica was connected to a flow loop which comprised a peristaltic roller pump used to deliver an oscillatory flow of saline solution, with peripheral resistance provided by adjustable clamps and the flow through each segment was calibrated to mimic cerebral hemodynamics. A filter funnel (51 microns filter) was attached to the saline reservoir. A pulsatile pressure waveform similar to those observed in the human carotid arteries was generated by the pump.³⁴ Flow and pressure were measured using flow Sensors (Transonic Systems Inc., Ithaca, NY) and pressure transducers (Validyne Engineering, Northridge, CA) attached to the MCA and ACA. The data acquisition system was equipped with an analog-to-digital converter, and incorporated the synchronized video captured by a digital camcorder.

3.4 *Flow restoration procedure and distal emboli analysis*

jnis-2022-019779-R1

Prior to initiating thrombectomy, complete vessel occlusion with TICI 0 was confirmed. In the event that TICI > 0 was observed, the experiment was halted, the clot was removed, and the system was flushed before new clot placement. The experiment was excluded for analysis in cases of malposition of the clot (internal carotid artery or distal M2 segment) and if the clot was fragmented on delivery prior to MT. Co-aspiration was used during clot retrieval for all thrombectomy procedures as described above.

3.5 Flow restoration procedure

All MT procedures were performed by an experienced neuro-interventional radiologist (V.A.) blinded to the device type. Briefly, a long sheath (Neuron Max 0.088 in, Penumbra, Alameda CA) was placed in the ICA and an aspiration catheter (Catalyst 5F, Stryker Neurovascular, Fremont CA) was then advanced up to the terminal ICA. AA Rebar 18 microcatheter (Medtronic) was placed over a 0.014" micro guidewire (Synchro, Stryker) and was positioned to the distal end of the occlusive clot. The guide wire was then withdrawn and replaced by the MT device. Each device was deployed at the occlusion site per the manufacturer's instructions. Each device remained in place for three minutes before retrieval. The MT device supported by the microcatheter were then withdrawn slowly until the entrance into the aspiration catheter. This step ended when the backflow into the aspiration tubing stopped. Then the triaxial system (aspiration catheter, microcatheter, device) was locked and retrieved slowly as a whole. Additional aspiration was applied via a syringe for the duration of device pull back into the long sheath to avoid any effect from stripping the clot off the device. One device was used per experiment for a maximum of three passes. Fluoroscopic and direct visualization of the model was used to determine the modified TICI score. Angiography was not performed since the use of contrast would interfere with the particulate count.

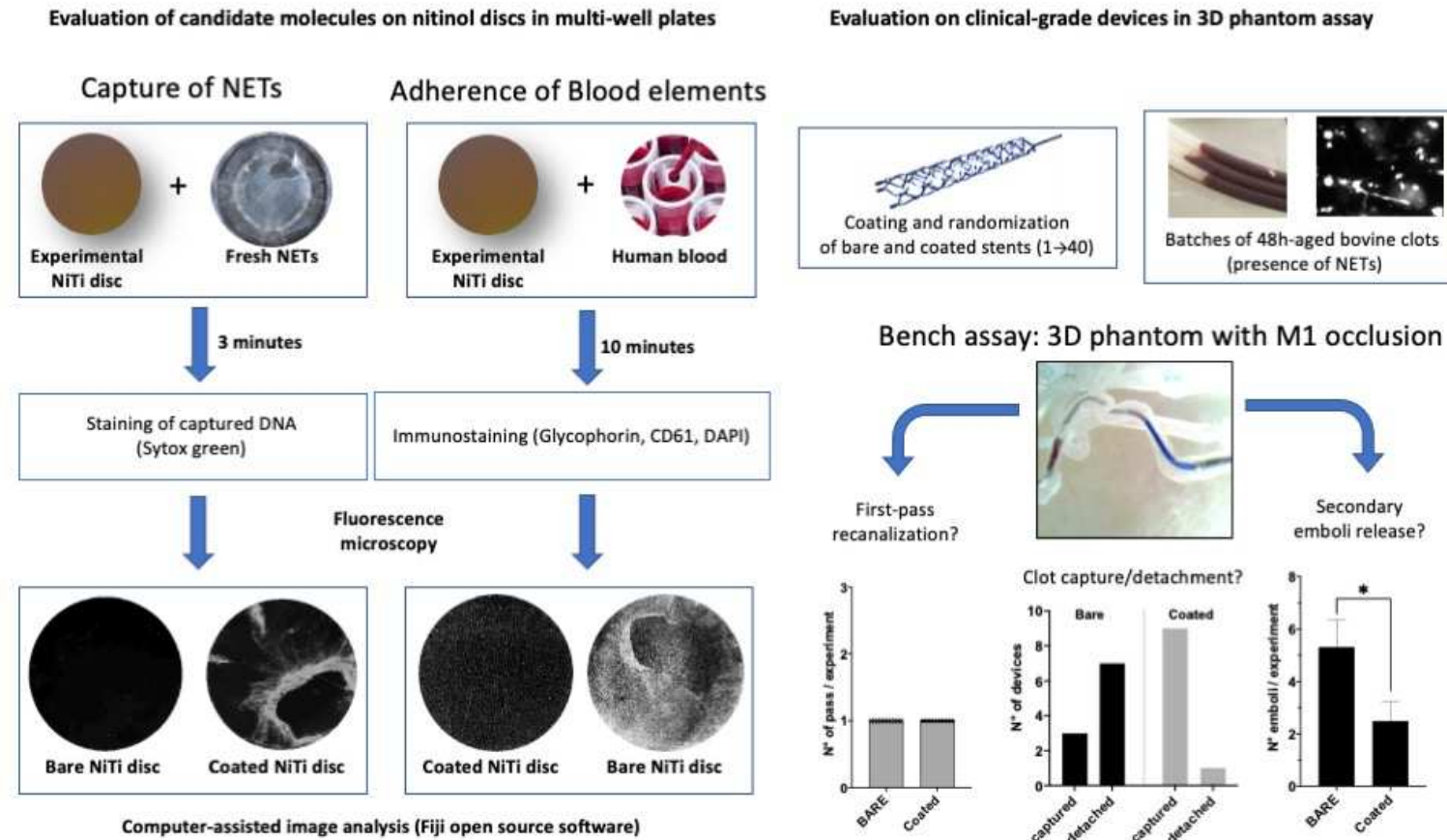
3.6 Particulate analysis for distal emboli

jnis-2022-019779-R1

Prior to each experiment, a 500 ml blank specimen was collected to measure particulate matter unassociated with the thrombectomy procedure. Particle collection began immediately prior to device deployment and ended after clot removal. Clot fragments generated during MT were washed into two collection reservoirs (one for emboli to the MCA distribution and the other to the ACA distribution) for further analysis. First, particulates greater than 1,000 μm were manually separated from the collection chamber and measured with calipers. The Coulter Principle was used to characterize particulates with sizes ranging from 200 to 1,000 μm (Multisizer 4 Coulter Counter, Beckman Coulter, Inc., Brea, CA). The particle size distribution of the blank specimen was subtracted from that measured following the thrombectomy experiment.

Supplemental information S 1

Overall strategy

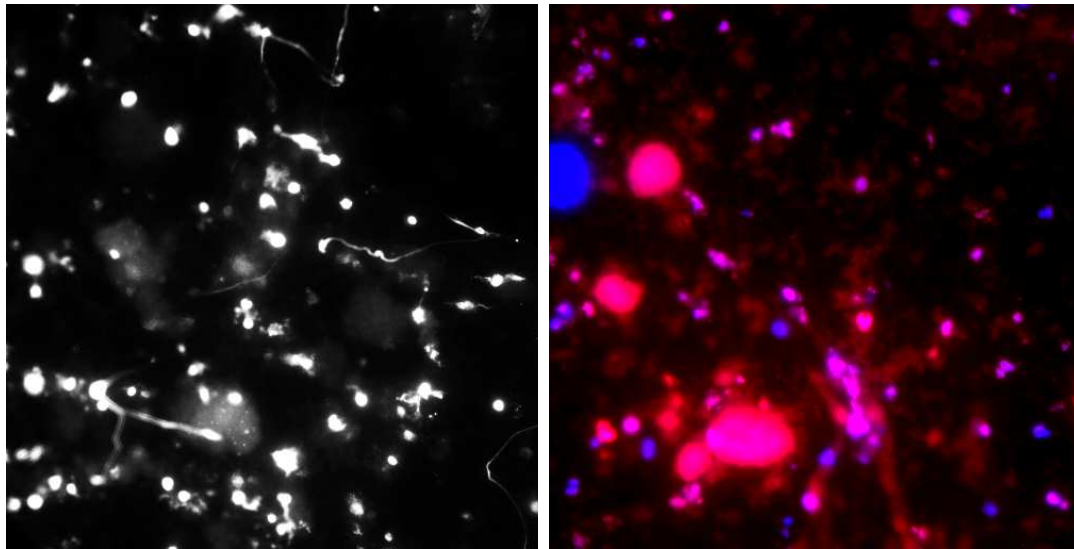


jnis-2022-019779-R1

Supplemental information S 2

Detection of extracellular DNA meshes in cryosections of the 48h-aged bovine blood clots used for functional testing of experimental devices in the 3D phantom assay.

Left: DAPI staining alone, extracellular DNA is detectable as faint large halos and long filaments. Right: the extracellular DNA (DAPI, blue) reflect the active release of extracellular traps (NETs) by nucleated cells, as detected by the associated citrullinated histones (H3cit immunostaining, red).



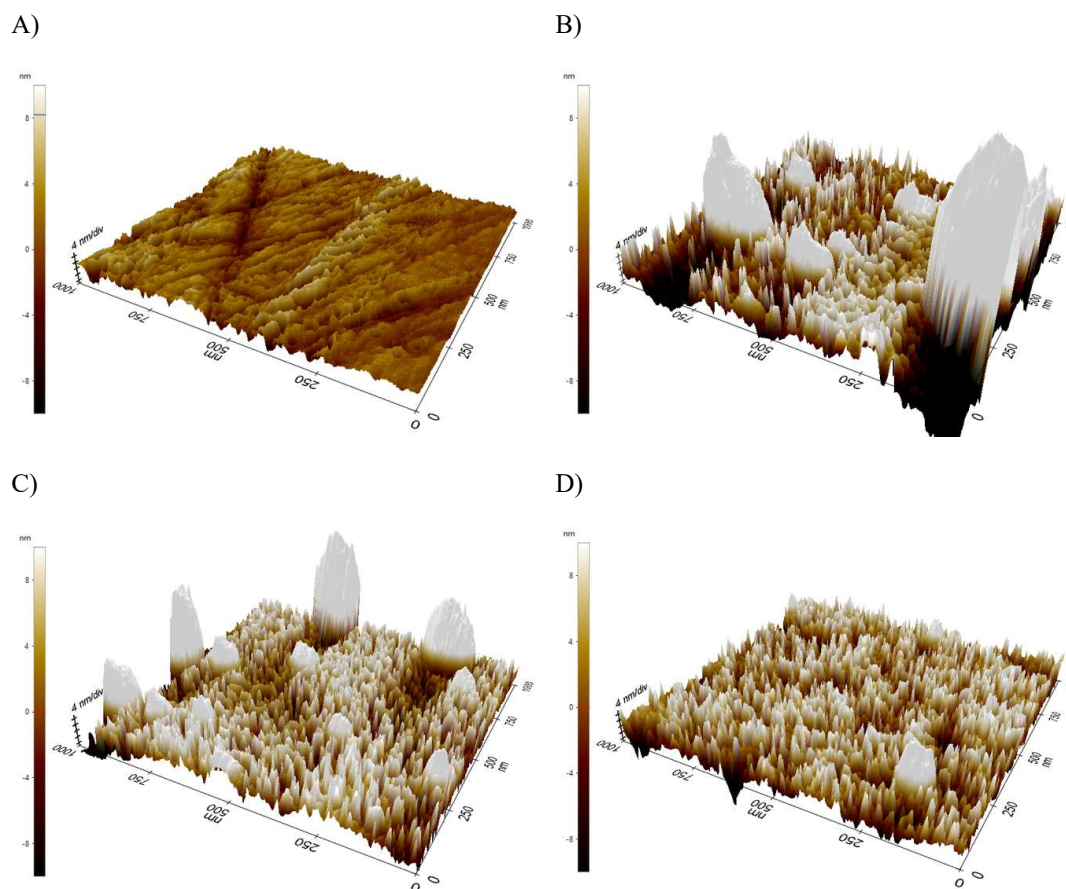
jnis-2022-019779-R1

Supplemental information S 3

Characterization of sonicated experimental flat discs.

3D AFM images of the upper surface of (A) unmodified (bare) NiTi sample, (B) NiTi grafted by dip-coating with PDA, (C) NiTi grafted by serial dip-coating with PDA and DBCO, (D) NiTi grafted by serial dip-coating with PDA, DBCO, and one of the DNA ligands. NiTi: Nitinol, PDA: Polydopamine, DBCO: Dibenzocyclooctyne. Analyses were performed in air at 20° C on 1 μm^2 areas.

Please note that the aggregates generated at the surface of PDA film (B) are consistently reduced by the subsequent grafting steps (C and D) and the surface of fully functionalized samples appears as smooth and very thin (D). Representative example of 3 independent experiments.



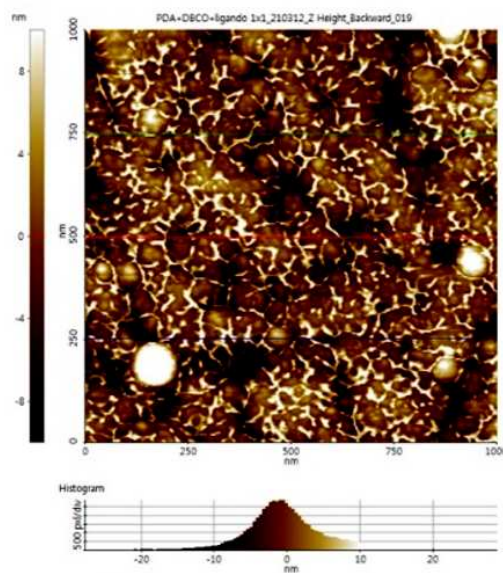
jnis-2022-019779-R1

Supplemental information S 4

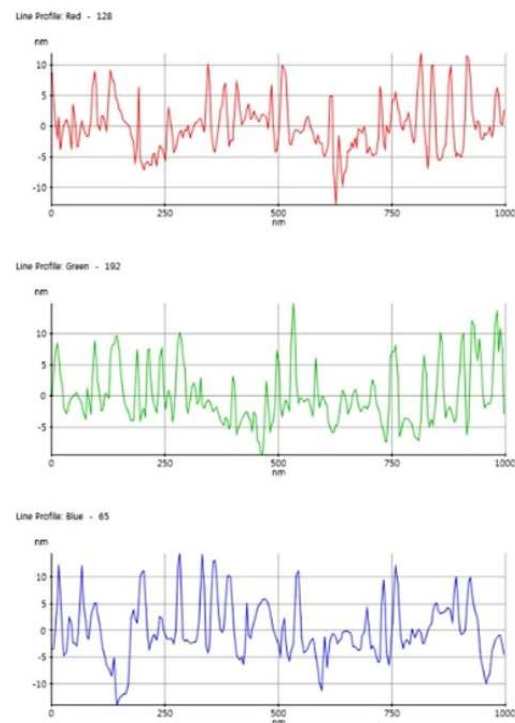
Surface roughness analysis on fully functionalized flat samples. (A) Representative 2D AFM image (1 μm^2) of a NiTi disc serially grafted with PDA, DBCO, and a DNA Ligand; (B) Profile of three different channels (Red, Green and blue). (C) Exemple of Skewness (Rsk) and Kurtosis (Rku) values, calculated on the three profiles.

NiTi: Nitinol, PDA: Polydopamine, DBCO: Dibenzocyclooctyne.

A)



B)



C)

Line	Rsk	Rku
Red	-0,478	3,211
Green	-0,829	3,113
Blue	-0,303	3,203

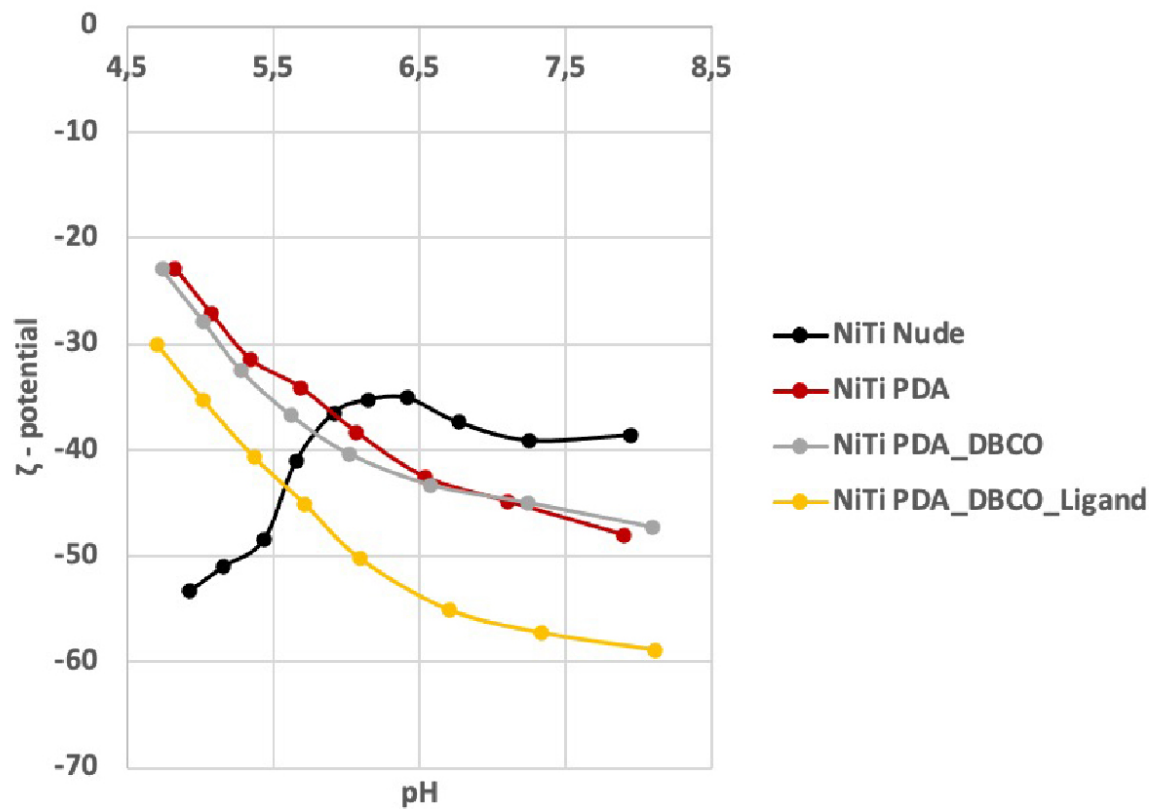
jnis-2022-019779-R1

Supplemental information S 5

Zeta potential analysis of experimental flat surfaces. Data were generated by a pH scan analysis of 4 groups of NiTi samples (n=3/group).

NiTi Nude: unmodified NiTi surface, NiTi PDA: NiTi surface coated with PDA alone; NiTi PDA_DBCO: NiTi surface grafted with PDA followed by grafting with DBCO; NiTi PDA_DBCO_Ligand: fully funzionalized sample.

NiTi: Nitinol, PDA: Polydopamine, DBCO: Dibenzocyclooctyne.



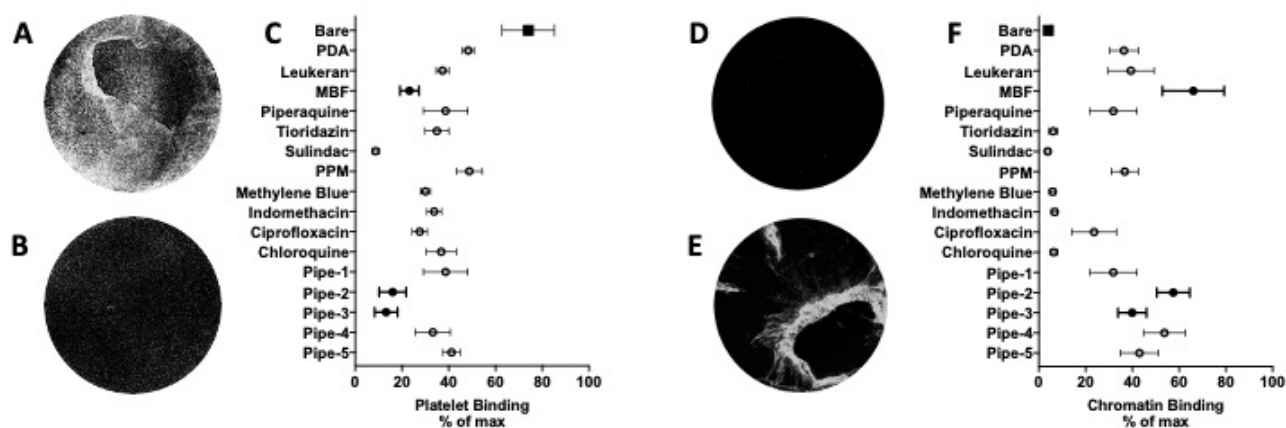
jnis-2022-019779-R1

Supplemental information S 6

Quantification by fluorescent staining of elements stably adhering onto experimental discs upon contact with human blood vs fresh NETs (as illustrated in supplementary information S1). Images were acquired by an inverted fluorescence microscope on the whole disc, positive surface was analyzed by batch analysis using the Fiji open on each disc from 15 different experimental groups (n=8/group) and data are expressed as % of max.

Example of platelet detection (CD61 immunofluorescent signal) on the surface of a bare (A) and of a Pipe-2 functionalized (B) NiTi disc;

Platelet adherence to NiTi discs was reduced by all type of coating (C). On the contrary, the adherence of extracellular chromatin upon contact with fresh NETs, was virtually absent on bare samples (D) and variably detectable on coated disc (E). Interestingly, the DNA-binding properties of piperazine were enhanced by specific linkers (Pipe-2 and Pipe-4). The best hits (MBF and Pipe-2) were identified as those combining a low binding to platelet and a high chromatin binding property.



jnis-2022-019779-R1

Supplemental information S 7

Clot removal in 3D phantom functional assays with unmodified solitaire devices (A) or devices coated with PDA alone (B) as compared to devices fully functionalized with MBF (C) or Pipe-2 (D). From left to right and for each experiment: stent deployment at site of occlusion, initiation of retrieval where the aspiration catheter engages the proximal clot surface, stent with clot during retrieval proximal to the ICA-cavernous segment, and re-sheathing. Most often the clot completely detached from BMS at the end of the retrieval and the TICI 3 recanalization score could only be achieved by the aspiration of the main clot into the guiding catheter (A). During retrieval with coated stents, clot fragmentation was observed but the clot fragments remained in contact with the stent-struts until complete entrance of the device into the guiding catheter. BMS: Bare metal stent, PDA: Polydopamine, MBF: Mustard benzo[b]furan, a DNA mustard derivative, Pipe-2: Piperazine derivative.

